

Supporting Information for:

**Structure and Dynamics of Water at Water-Graphene and  
Water-Hexagonal Boron-Nitride Sheet Interfaces  
Revealed by *Ab initio* Sum-Frequency Generation  
Spectroscopy**

**Tatsuhiko Ohto<sup>1\*</sup>, Hirokazu Tada<sup>1</sup>, and Yuki Nagata<sup>2\*</sup>**

1. Graduate School of Engineering Science, Osaka University, 1-3 Machikaneyama,  
Toyonaka, Osaka, 560-8531, Japan
2. Max-Planck Institute for Polymer Research, Ackermannweg 10, 55128, Mainz,  
Germany

email: [ohito@molelectronics.jp](mailto:ohito@molelectronics.jp), [nagata@mpip-mainz.mpg.de](mailto:nagata@mpip-mainz.mpg.de)

**Contents:**

- I. Density Profile of Water near Graphene and hexagonal Boron-Nitride (hBN)
- II. Simulation Protocols for SFG Spectra
- III. Dangling O-D Group Definition
- IV. Structural Order of the First Layer Water

## I. Density Profile of Water near Graphene and hexagonal Boron-Nitride (hBN)

Figure S1 shows the axial profiles of water density at the water-graphene and water-BN interfaces. Both profiles are similar and are characterized by two peaks; the first and second peaks are located at  $z = \sim 3 \text{ \AA}$  with the height of  $\sim 2.1 \text{ g/cm}^3$  and at  $z = \sim 6 \text{ \AA}$  with  $\sim 1.5 \text{ g/cm}^3$ , respectively. Here, the  $z$ -axis forms the surface normal and the origin point of the  $z$ -axis is given by the position of the graphene/BN density maximum. The similar water density profiles at the graphene and hBN interfaces are consistent with the previous report,<sup>1</sup> while the peak height of the first peak of  $3.7 \text{ g/cm}^3$  differs significantly from our results. This difference in the peak height can be attributed to the different exchange-correlation functional and the van der Waals correction method (optB88-vdW<sup>2-3</sup> in Ref. 1 and BLYP-D3 in our work). Here, we note that the optB88-vdW tends to overestimate the absorption energy of water on the graphene,<sup>1</sup> while the BLYP+D3 provides good agreement of the simulated SFG spectra with the experimental spectra<sup>4</sup> as well as the surface tension of water at the water-air interface.<sup>5</sup> It has been also reported that the BLYP+D3 reproduces the same stability of water near the hBN sheet to the optB88-vdW functional,<sup>6</sup> indicating that BLYP-D3 is appropriate to describe the weak interaction between the 2D sheets and water. Finally, the  $6 \times 10$  orthorhombic cell used in our calculations is a sufficient size to reproduce the electronics structure of graphene and hBN only with the Gamma point.<sup>1</sup>

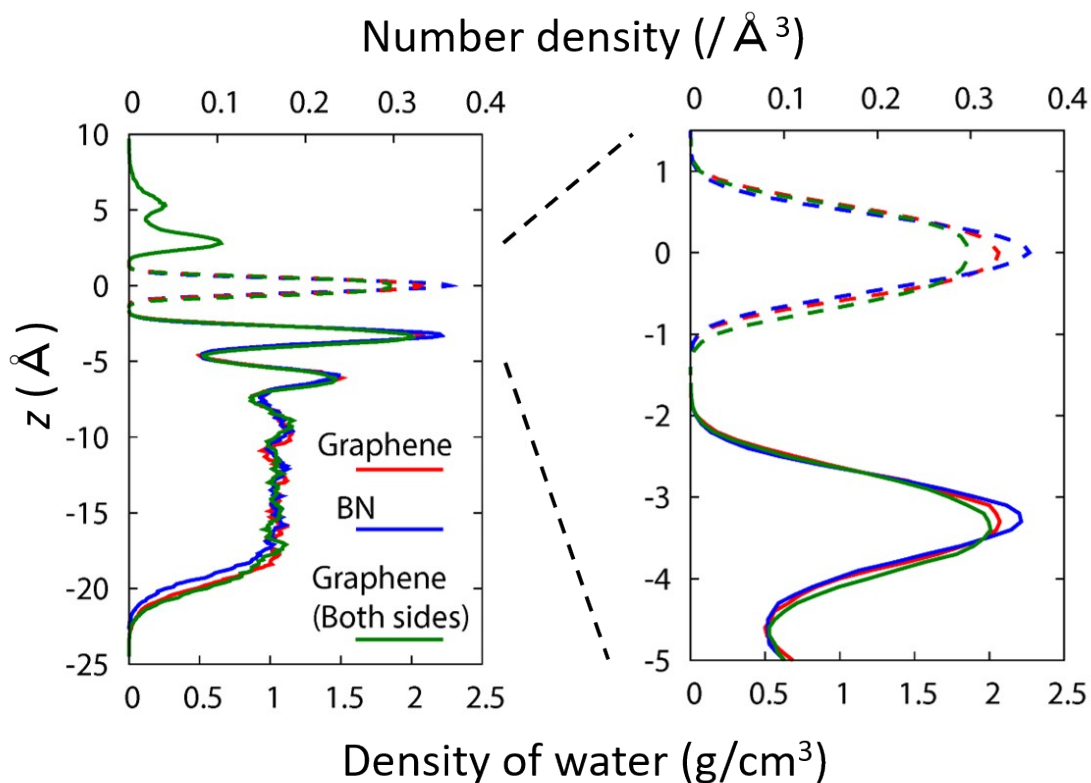


**Figure S1.** Axial profiles of the density of water (solid lines) as well as the number density of C and B/N and N atoms of graphene and hBN, respectively (dashed lines). In these profiles, the heavy water ( $D_2O$ ) molecules used in the MD simulations were considered as the  $H_2O$ . The origin point is given by the graphene/BN sheet position.

## II. Simulation Protocols for SFG Spectra

We used the surface-specific velocity-velocity correlation function (ssVVCf) algorithm,<sup>4</sup>

where the resonant part of the SFG response function,  $\chi_{xxz}^{(2),R}(\omega)$  can be written as:

$$\chi_{xxz}^{(2),R}(\omega) = \frac{Q(\omega)\mu'(\omega)\alpha'(\omega)}{i\omega^2} \chi_{xxz}^{ssVVAF}(\omega), \quad (S1)$$

$$\chi_{xxz}^{ssVVCf}(\omega) = \int_0^{\infty} dt e^{-i\omega t} \left\langle \sum_{ij} g_{ds}(z_i(0)) \dot{r}_{z,i}^{OD}(0) \frac{\vec{r}_j^{OD}(t) \cdot \dot{\vec{r}}_j^{OD}(t)}{|\dot{\vec{r}}_j^{OD}(t)|} \right\rangle. \quad (S2)$$

$z_i(t)$  is the z-coordinate of the  $i$ th oxygen atom at time  $t$ , and  $g_{ds}(z_i)$  is the function for the dividing surface to selectively extract the vibrational responses of D<sub>2</sub>O molecules near the interface. For the D<sub>2</sub>O-graphene interface and D<sub>2</sub>O-BN interface, we used

$$g_{ds}(z_i) = \begin{cases} 1 & \text{for } -9 \text{ \AA} \leq z_i \\ 0 & \text{for } z_i < -9 \text{ \AA} \end{cases}. \quad (S3)$$

where  $z_{ds}$  is the z-coordinate of the dividing surface and. For the D<sub>2</sub>O-air interface, we used

$$g_{ds}(z_i) = \begin{cases} 1 & \text{for } z_i < -13 \text{ \AA} \\ 0 & \text{for } -13 \text{ \AA} \leq z_i \end{cases}. \quad (S4)$$

For the penetrated water cases on the graphene interface, we used.

$$g_{ds}(z_i) = \begin{cases} 0 & \text{for } z_i < 0 \text{ \AA} \\ 1 & \text{for } 0 \text{ \AA} \leq z_i < 4.5 \text{ \AA} \\ 0 & \text{for } 4.5 \text{ \AA} \leq z_i \end{cases}. \quad (S5)$$

Such  $z_{ds}$  are schematically depicted in Figure S2. The criterion of  $z = 4.5 \text{ \AA}$  for the penetrated water was selected to include the topmost water layer near the graphene (see Figure S1). This is rationalized by the fact the thickness for the corrugated graphene is sub-nm scale.<sup>7-9</sup>

In this study, we consider the case that the O-D stretch chromophores are decoupled from the other O-D chromophores. This corresponds to the situation of isotopically diluted water (H-O-D in D<sub>2</sub>O). When the O-D stretch chromophores are isolated, the cross-correlation term in Equation (S2) is zero and thus Equation (S2)

reduced to the surface-specific autocorrelation function (ssVAF) as:

$$\chi_{xxz}^{ssVAF}(\omega) = \int_0^{\infty} dt e^{-i\omega t} \left\langle \sum_i g_{ds}(z_i(0)) \dot{r}_{z,i}^{OD}(0) \frac{\vec{r}_i^{OD}(t) \cdot \vec{r}_i^{OD}(t)}{|\vec{r}_i^{OD}(t)|} \right\rangle. \quad (S6)$$

The induced dipole moment due to the surrounding water molecules (solvation effects) are included through the frequency dependent transition dipole moment ( $\mu'(\omega)$ ) and polarizability ( $\alpha'(\omega)$ ):<sup>10-11</sup>

$$\mu'(\omega) \equiv \left( 1.377 + \frac{53.03(2745.8 - \omega)}{4870.3} \right) \mu^0, \quad (S7)$$

$$\alpha'(\omega) \equiv \left( 1.271 + \frac{5.287(2745.8 - \omega)}{4870.3} \right) \alpha^0, \quad (S8)$$

where  $\omega$  is in  $\text{cm}^{-1}$ .  $Q(\omega)$  is the quantum correction factor given by:<sup>12</sup>

$$Q(\omega) = \frac{\beta \hbar \omega}{1 - \exp(-\beta \hbar \omega)}, \quad (S9)$$

where  $\beta = 1/kT$  is the inverse temperature.

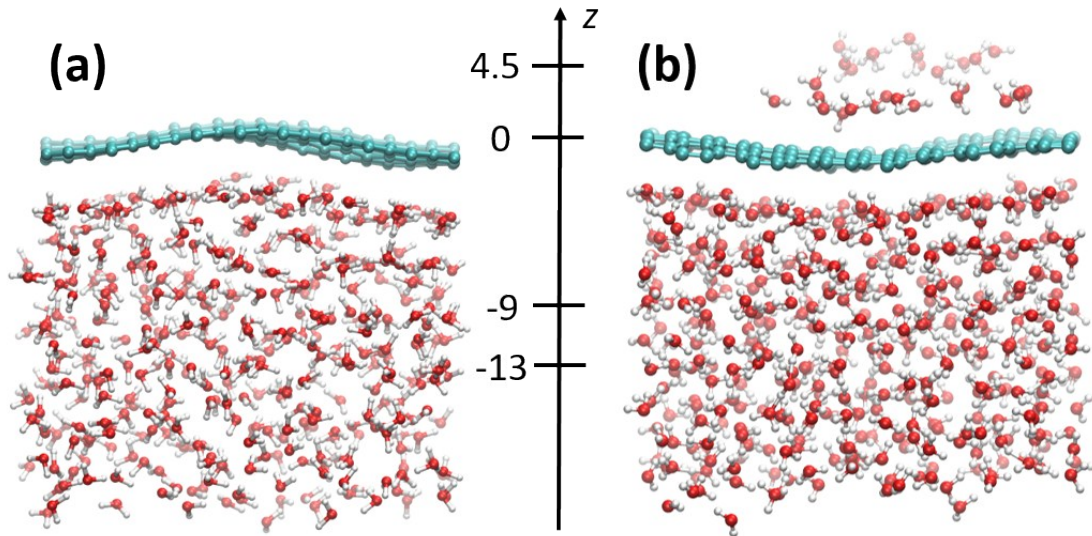


**Figure S2.** Snapshots of water-graphene interfaces. Water molecules exist (a) down side

only and (b) both sides of graphene. The water-molecules

### III. Dangling O-D Group Definition

The H-bond of water is defined based on the water dimer conformation shown in Fig. S4(d). Here,  $R$  and  $r$  are the intermolecular O...O and O...D distances of water dimer, respectively.  $\beta$  and  $\theta$  denote the angles of D-O...O and O-D...O, respectively, while  $\psi$  is the angle formed by the O...D vector and the plane formed by H-O-D atoms. It has been already shown using the POLI2VS water model<sup>13</sup> that the  $R$ - $\theta$  definition is the most appropriate to define the free O-H groups at the water-air surface.<sup>14</sup> We calculated the SFG spectra with the criteria of  $(R_c, \theta_c) = (3.5 \text{ \AA}, 110^\circ)$ , where  $R_c$  and  $\theta_c$  are the critical distance and angle, respectively. Figs S3(a)-(c) show that the free OD groups are captured well with the  $R$ - $\theta$  definition, even at the water-graphene and water-hBN interfaces based on AIMD simulations.

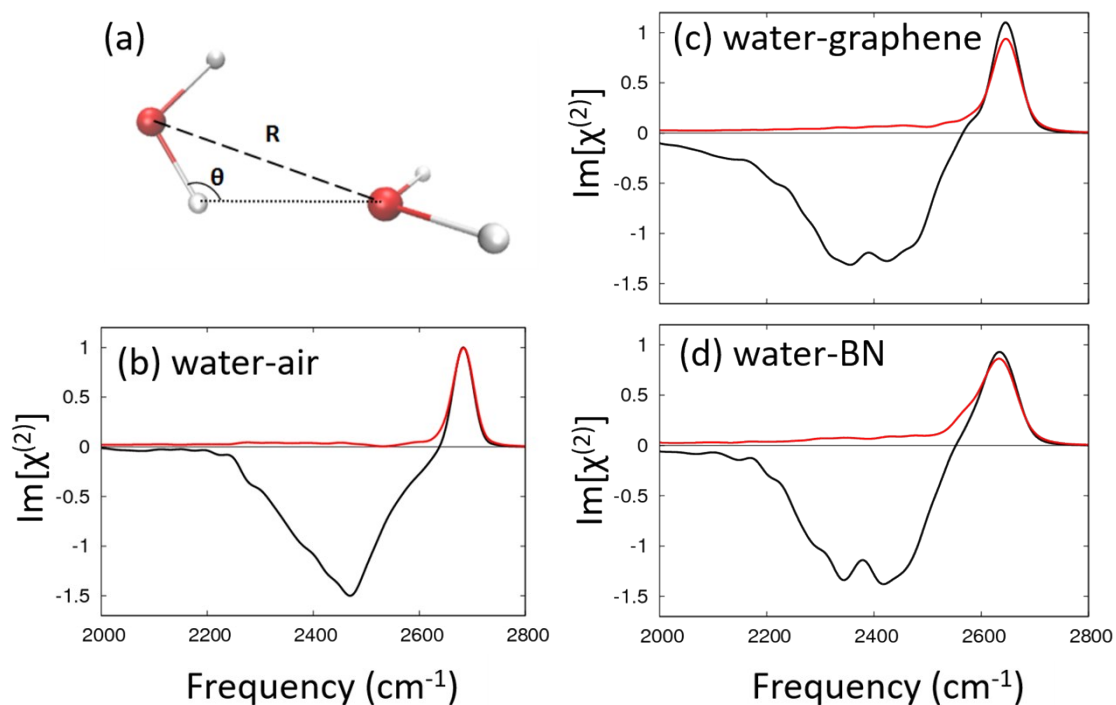


**Figure S3.** (a) Schematic of the heavy water dimer conformation, the O...D distances  $R$  the O...O-D angles  $\beta$  for defining the free O-D group. A red (white) sphere represents a D atom. SFG spectra of the isotopically diluted O-D stretch mode at the (b) water-air, (c) water-graphene, and (d) water-BN interfaces. The black lines represent the total spectra and the red lines represent the contributions from the dangling O-D group defined using  $(R_c, \theta_c) = (3.5 \text{ \AA}, 110^\circ)$ .

#### IV. Structural Order of the First Layer Water

Figure S4 shows the two-dimensional position probability of D atom in the first layer of water molecules ( $-5 \text{ \AA} < z < 0 \text{ \AA}$  in Figure S1). D atoms distribute slightly localized on the ring at the graphene, while they are localized on the N atoms of hBN in the first layer of water ranging over  $5 \text{ \AA}$ . Our data support the large friction of water molecules at the water-BN sheet interface.<sup>1</sup>

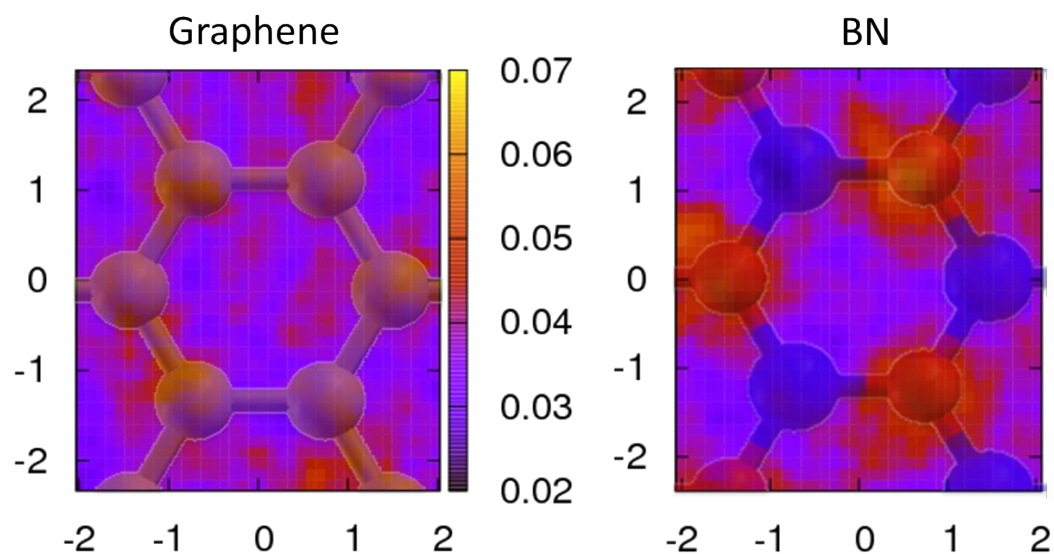


**Figure S4.** Position probability of D atoms of  $D_2O$  molecules near the graphene and hBN interface. We used the  $D_2O$  atom within the first layer of water.

## References

1. Tocci, G.; Joly, L.; Michaelides, A., Friction of Water on Graphene and Hexagonal Boron Nitride from Ab Initio Methods: Very Different Slippage Despite Very Similar Interface Structures. *Nano Lett.* **2014**, *14*, 6872-6877.
2. Klimes, J.; Bowler, D. R.; Michaelides, A., Chemical Accuracy for the Van Der Waals Density Functional. *J. Phys.: Condens. Matter* **2010**, *22*, 022201.
3. Klimeš, J.; Bowler, D. R.; Michaelides, A., Van Der Waals Density Functionals Applied to Solids. *Phys. Rev. B* **2011**, *83*, 195131.
4. Ohto, T.; Usui, K.; Hasegawa, T.; Bonn, M.; Nagata, Y., Toward Ab Initio Molecular Dynamics Modeling for Sum-Frequency Generation Spectra; an Efficient Algorithm Based on Surface-Specific Velocity-Velocity Correlation Function. *J. Chem. Phys.* **2015**, *143*, 124702.
5. Nagata, Y.; Ohto, T.; Bonn, M.; Kuhne, T. D., Surface Tension of Ab Initio Liquid Water at the Water-Air Interface. *J. Chem. Phys.* **2016**, *144*, 204705.
6. Kayal, A.; Chandra, A., Orientational Order and Dynamics of Interfacial Water near a Hexagonal Boron-Nitride Sheet: An Ab Initio Molecular Dynamics Study. *J. Chem. Phys.* **2017**, *147*,

164704.

7. Fasolino, A.; Los, J. H.; Katsnelson, M. I., Intrinsic Ripples in Graphene. *Nat. Mater.* **2007**, *6*, 858-861.
8. Geringer, V.; Liebmann, M.; Echtermeyer, T.; Runte, S.; Schmidt, M.; Ruckamp, R.; Lemme, M. C.; Morgenstern, M., Intrinsic and Extrinsic Corrugation of Monolayer Graphene Deposited on SiO<sub>2</sub>. *Phys. Rev. Lett.* **2009**, *102*, 076102.
9. Voloshina, E.; Dedkov, Y., Atomic Force Spectroscopy and Density-Functional Study of Graphene Corrugation on Ru(0001). *Phys. Rev. B* **2016**, *93*, 235418.
10. Auer, B. M.; Skinner, J. L., Ir and Raman Spectra of Liquid Water: Theory and Interpretation. *J. Chem. Phys.* **2008**, *128*, 224511.
11. Corcelli, S. A.; Skinner, J. L., Infrared and Raman Line Shapes of Dilute H<sub>2</sub>O in Liquid H<sub>2</sub>O and D<sub>2</sub>O from 10 to 90 °C. *J. Phys. Chem. A* **2005**, *109*, 6154-6165.
12. Berens, P. H., Molecular Dynamics and Spectra. I. Diatomic Rotation and Vibration. *J. Chem. Phys.* **1981**, *74*, 4872.
13. Hasegawa, T.; Tanimura, Y., A Polarizable Water Model for Intramolecular and Intermolecular Vibrational Spectroscopies. *J. Phys. Chem. B* **2011**, *115*, 5545-5553.
14. Tang, F.; Ohto, T.; Hasegawa, T.; Xie, W. J.; Xu, L.; Bonn, M.; Nagata, Y., Definition of Free O-H Groups of Water at the Air-Water Interface. *J. Chem. Theor. Comput.* **2018**, *14*, 357-364.